Influence of In-Plane Shear Nonlinearity on Buckling and Postbuckling Responses of Composite Plates and Shells

HSUAN-TEH HU
Department of Civil Engineering
National Cheng Kung University
1 University Road
Tainan, Taiwan
Republic of China

(Received November 1, 1991)
(Revised June 18, 1992)

ABSTRACT: Based on linear and nonlinear in-plane shear formulations for fiber-composite laminate materials, finite-element buckling analyses for composite plates under uniaxial compression and biaxial compression and for composite shells under end compression and hydrostatic compression are presented. It has been shown that the nonlinear in-plane shear has significant influence on the buckling and postbuckling responses of composite plates and shells, specially for those with $[45/-45]_{2s}$ layup.

KEY WORDS: in-plane shear nonlinearity, buckling, postbuckling, finite element, composite plates, composite shells.

INTRODUCTION

THE USE OF fiber reinforced composite laminate materials in aircraft and aerospace structures has increased rapidly in recent years. While composite materials offer many desirable structural properties over conventional materials, they also pose challenging technical problems in understanding their buckling and postbuckling responses. In the literature, most stability studies of fiber-composite laminate plates and shells have been limited to the geometrically nonlinear analysis [1–4]. Little attention has been paid to the material nonlinearity. It is well known that unidirectional fibrous composites exhibit severe nonlinearity in in-plane shear stress-strain relation. In addition, deviation from linearity is also observed in in-plane transverse loadings; however, the degree of nonlinearity is not comparable to that in the in-plane shear [5].

Most existing macromechanical models for fiber-composite materials have been based on nonlinear elasticity [5–8], or plasticity [7,9–11]. Generally, the mechanical response of fiber-composite materials is very complicated. Since the

0021-9983/93/02 0138-14 $6.00/0

nonlinearity of in-plane shear is the most significant one for composite materials, the aim of this work is therefore focusing on the influence of in-plane shear nonlinearity on the buckling and postbuckling responses of composite laminate plates and shells.

In this investigation, nonlinear buckling analyses for simply supported composite plates under uniaxial compressive and biaxial compressive loads and for simply supported composite shells under end compressive and hydrostatic compressive loads are carried out using the ABAQUS finite element program [12]. Numerical results for the buckling and postbuckling responses of these composite structures with linear and nonlinear in-plane shear formulations are presented and discussed. Finally, important conclusions obtained from the study are given.

CONSTITUTIVE MODELLING OF LAMINA

For fiber-composite laminate materials, each lamina can be considered as an orthotropic layer in a plane stress condition. The incremental constitutive matrices for a linear orthotropic lamina in the material coordinates (Figure 1) can be written as

$$\Delta\{\sigma'\} = [Q_1']\Delta\{\epsilon'\} \qquad \Delta\{\tau_t'\} = [Q_2']\Delta\{\gamma_t'\} \tag{1}$$

$$[Q_1'] = \begin{bmatrix} \dfrac{E_{11}}{1-\nu_{12}\nu_{21}} & \dfrac{\nu_{12}E_{22}}{1-\nu_{12}\nu_{21}} & 0 \\ \dfrac{\nu_{21}E_{11}}{1-\nu_{12}\nu_{21}} & \dfrac{E_{22}}{1-\nu_{12}\nu_{21}} & 0 \\ 0 & 0 & G_{12} \end{bmatrix}, \quad [Q_2'] = \begin{bmatrix} \alpha_1 G_{13} & 0 \\ 0 & \alpha_2 G_{23} \end{bmatrix} \tag{2}$$

where $\Delta\{\sigma'\} = \Delta\{\sigma_1,\sigma_2,\tau_{12}\}^T$, $\Delta\{\tau_t'\} = \Delta\{\tau_{13},\tau_{23}\}^T$, $\Delta\{\epsilon'\} = \Delta\{\epsilon_1,\epsilon_2,\gamma_{12}\}^T$, $\Delta\{\gamma_t'\} = \Delta\{\gamma_{13},\gamma_{23}\}^T$ are incremental stress and strain components. The α_1 and α_2 are the shear correction factors [13] and are taken to be 0.83 in this study.

To model the nonlinear in-plane shear behavior, the nonlinear strain-stress relation for a composite lamina suggested by Hahn and Tsai [5] is adopted in this study, which is given as follows:

$$\begin{Bmatrix} \epsilon_1 \\ \epsilon_2 \\ \gamma_{12} \end{Bmatrix} = \begin{bmatrix} \dfrac{1}{E_{11}} & -\dfrac{\nu_{21}}{E_{22}} & 0 \\ -\dfrac{\nu_{12}}{E_{11}} & \dfrac{1}{E_{22}} & 0 \\ 0 & 0 & \dfrac{1}{G_{12}} \end{bmatrix} \begin{Bmatrix} \sigma_1 \\ \sigma_2 \\ \tau_{12} \end{Bmatrix} + S_{6666}\tau_{12}^2 \begin{Bmatrix} 0 \\ 0 \\ \tau_{12} \end{Bmatrix} \tag{3}$$

In this model only one material constant S_{6666} is required to account for the in-plane shear nonlinearity. The value of S_{6666} can be determined by a curve fit to various off-axis tension test data [5]. By inverting and differentiating Equation (3), the nonlinear incremental constitutive matrix for the lamina can be obtained as

$$[Q_1'] = \begin{bmatrix} \dfrac{E_{11}}{1 - \nu_{12}\nu_{21}} & \dfrac{\nu_{12}E_{22}}{1 - \nu_{12}\nu_{21}} & 0 \\ \dfrac{\nu_{21}E_{11}}{1 - \nu_{12}\nu_{21}} & \dfrac{E_{22}}{1 - \nu_{12}\nu_{21}} & 0 \\ 0 & 0 & \dfrac{1}{1/G_{12} + 3S_{6666}\tau_{12}^2} \end{bmatrix} \tag{4}$$

This nonlinear constitutive model for fiber-composite laminate materials is implemented into the ABAQUS finite element program as a user-defined material subroutine to carry out nonlinear buckling analyses.

CONSTITUTIVE MODELLING OF COMPOSITE SHELL SECTION

The elements used in the numerical analyses are eight-node isoparametric shells with six degrees of freedom per node (three displacements and three rotations). The formulation of the shell allows transverse shear deformation [12,14] and these shear flexible shells can be used for both thick and thin shell analysis [12].

During finite element analysis, the constitutive matrices of composite materials at element integration points must be calculated before the stiffness matrices are

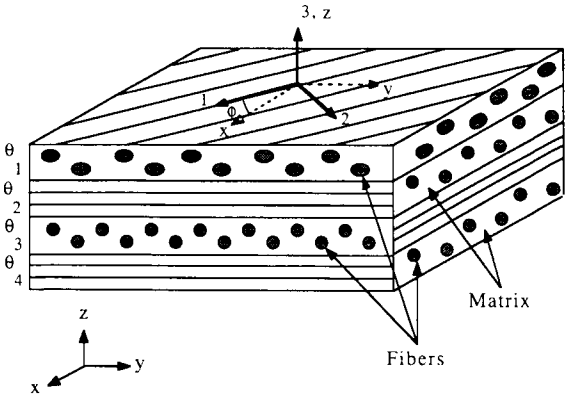

Figure 1. *Material and element coordinate systems for laminate composites.*

assembled from element level to structural level. The incremental constitutive equations for a lamina in the element coordinates (Figure 1) can be written as:

$$\Delta\{\sigma\} = [Q_1]\Delta\{\epsilon\} \qquad [Q_1] = [T_1]^T[Q_1'][T_1] \tag{5}$$

$$\Delta\{\tau_t\} = [Q_2]\Delta\{\gamma_t\} \qquad [Q_2] = [T_2]^T[Q_2'][T_2] \tag{6}$$

where $\Delta\{\sigma\} = \Delta\{\sigma_x,\sigma_y,\tau_{xy}\}^T$, $\Delta\{\tau_t\} = \Delta\{\tau_{xz},\tau_{yz}\}^T$, $\Delta\{\epsilon\} = \Delta\{\epsilon_x,\epsilon_y,\gamma_{xy}\}^T$, $\Delta\{\gamma_t\} = \Delta\{\gamma_{xz},\gamma_{yz}\}^T$, and

$$[T_1] = \begin{bmatrix} \cos^2\phi & \sin^2\phi & \sin\phi\cos\phi \\ \sin^2\phi & \cos^2\phi & -\sin\phi\cos\phi \\ -2\sin\phi\cos\phi & 2\sin\phi\cos\phi & \cos^2\phi - \sin^2\phi \end{bmatrix} \tag{7}$$

$$[T_2] = \begin{bmatrix} \cos\phi & \sin\phi \\ -\sin\phi & \cos\phi \end{bmatrix} \tag{8}$$

The ϕ is measured counterclockwise from the element local x-axis to the material 1-axis.

Assume $\Delta\{\epsilon_o\} = \Delta\{\epsilon_{xo},\epsilon_{yo},\gamma_{xyo}\}^T$ are the incremental in-plane strains at the mid-surface of the shell section and $\Delta\{\varkappa\} = \Delta\{\varkappa_x,\varkappa_y,\varkappa_{xy}\}^T$ are the incremental curvatures. The incremental in-plane strains, $\Delta\{\epsilon\} = \Delta\{\epsilon_x,\epsilon_y,\gamma_{xy}\}^T$, at a distance z from the mid-surface become

$$\Delta\{\epsilon\} = \Delta\{\epsilon_o\} + z\Delta\{\varkappa\} \tag{9}$$

Let h be the total thickness of the shell section, the incremental stress resultants, $\Delta\{N\} = \Delta\{N_x,N_y,N_{xy}\}^T$, $\Delta\{M\} = \Delta\{M_x,M_y,M_{xy}\}^T$ and $\Delta\{V\} = \Delta\{V_x, V_y\}$, can be defined as:

$$\begin{Bmatrix} \Delta\{N\} \\ \Delta\{M\} \\ \Delta\{V\} \end{Bmatrix} = \int_{-h/2}^{h/2} \begin{Bmatrix} \Delta\{\sigma\} \\ z\Delta\{\sigma\} \\ \Delta\{\tau_t\} \end{Bmatrix} dz = \int_{-h/2}^{h/2} \begin{Bmatrix} [Q_1](\Delta\{\epsilon_o\} + z\Delta\{\varkappa\}) \\ z[Q_1](\Delta\{\epsilon_o\} + z\Delta\{\varkappa\}) \\ [Q_2]\Delta\{\gamma_t\} \end{Bmatrix} dz$$

$$= \int_{-h/2}^{h/2} \begin{bmatrix} [Q_1] & z[Q_1] & [0] \\ z[Q_1] & z^2[Q_1] & [0] \\ [0]^T & [0]^T & [Q_2] \end{bmatrix} \begin{Bmatrix} \Delta\{\epsilon_o\} \\ \Delta\{\varkappa\} \\ \Delta\{\gamma_t\} \end{Bmatrix} dz \tag{10}$$

where [0] is a 3 by 2 matrix with all the coefficients equal to zero.

For a material nonlinear case, $[Q_1']$ matrix in Equation (5) is taken from Equation (4) and the incremental stress resultants of Equation (10) can be obtained by a numerical integration through the thickness of composite shell section. For a material linear case, $[Q_1']$ matrix used in Equation (5) is taken from Equation (2)

and the incremental stress resultants of shell section can be written as a summation of integrals over the n laminae in the following form:

$$\begin{Bmatrix} \Delta\{N\} \\ \Delta\{M\} \\ \Delta\{V\} \end{Bmatrix} = \left(\sum_{j=1}^{n} \begin{bmatrix} (z_{jt} - z_{jb})[Q_1] & \frac{1}{2}(z_{jt}^2 - z_{jb}^2)[Q_1] & [0] \\ \frac{1}{2}(z_{jt}^2 - z_{jb}^2)[Q_1] & \frac{1}{3}(z_{jt}^3 - z_{jb}^3)[Q_1] & [0] \\ [0]^T & [0]^T & (z_{jt} - z_{jb})[Q_2] \end{bmatrix} \right) \begin{Bmatrix} \Delta\{\epsilon_o\} \\ \Delta\{\chi\} \\ \Delta\{\gamma_t\} \end{Bmatrix} \tag{11}$$

where z_{jt} and z_{jb} are distances from the mid-surface of the section to the top and the bottom of the jth layer respectively.

NONLINEAR FINITE ELEMENT ANALYSIS

In the ABAQUS finite element program, the nonlinear response of a structure is modeled by an updated Lagrangian formulation and a modified Riks nonlinear incremental algorithm [15] can be used to construct the equilibrium solution path. To model bifurcation from the prebuckling path to the postbuckling path, geometric imperfections of composite plates and shells are introduced by superimposing a small fraction (say 0.001 of the plate thickness or shell thickness) of the lowest eigenmode determined by a linearized buckling analysis to the original nodal coordinates of plates or shells.

NUMERICAL ANALYSES

Composite Plates under Uniaxial Compression

In this section, square composite plates with different laminate layups, $[90/0]_{2S}$, $[45/-45/90/0]_S$ and $[45/-45]_{2S}$, are analyzed. The thickness of each ply is 0.159 cm (0.0625 in.). Ply constitutive properties and plate geometries are given in Figure 2. The linear and nonlinear in-plane shear stress-strain curves are shown in Figure 3. These plates are subjected to uniform uniaxial compressive loads in the x direction. The edges of these plates are simply supported, which prevents out of plane motions but allows in-plane movements in x and y directions.

To estimate the buckling loads and to generate geometric imperfections for composite plates, linearized buckling analyses are carried out. The linearized buckling loads N_{xcr} and buckling modes are shown in Figure 4. All plates buckle into a half-wave in the x direction and a half-wave in the y direction.

The load-displacement curves of composite plates with the linear in-plane

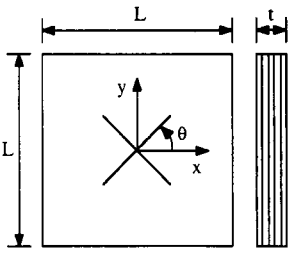

Laminate layups:
$[90/0]_{2S}$
$[45/-45/90/0]_S$
$[45/-45]_{2S}$

Composite plate geometry:
L = 10.16 cm (4 in.)
t = 1.27 cm (0.5 in.)

Ply constitutive properties:
E_{11} = 138 GPa
E_{22} = 14.5 GPa
$G_{12} = G_{13}$ = 5.86 GPa
G_{23} = 3.52 GPa
ν_{12} = 0.21
S_{6666} = 7.32 $(GPa)^{-3}$

Figure 2. *Geometries and material properties for composite laminate plate.*

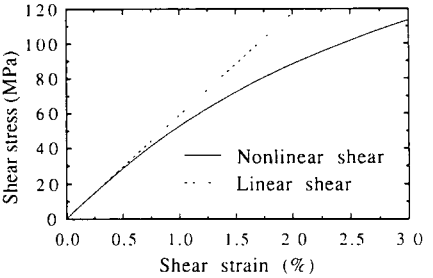

Figure 3. *In-plane shear stress-strain curves for composite lamina.*

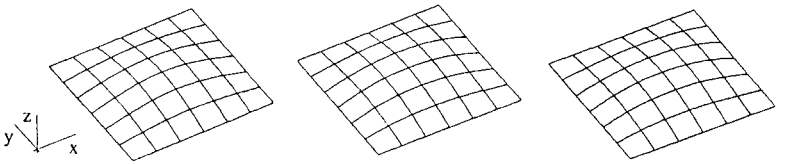

N_{xcr} = 219.9 kN/cm
$[90/0]_{2S}$ layup

N_{xcr} = 253.9 kN/cm
$[45/-45/90/0]_S$ layup

N_{xcr} = 253.8 kN/cm
$[45/-45]_{2S}$ layup

Figure 4. *Critical buckling loads and buckling modes for composite plates under uniaxial compression.*

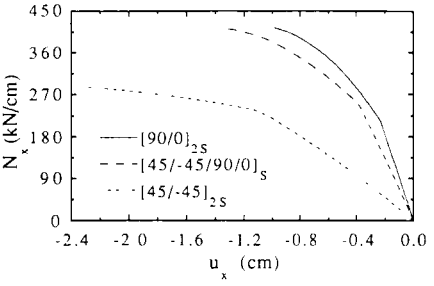

Figure 5. *Load-displacement curves for composite plates under uniaxial compression with linear in-plane shear formulation.*

shear formulation are plotted in Figure 5. The N_x is the uniform compressive force (positive value means compression) applied to the ends normal to the x direction and u_x is the associated end displacement (positive value means end extension and negative value means end shortening). This figure shows that the plate with $[90/0]_{2S}$ layup has the highest prebuckling and postbuckling stiffnesses and the plate with $[45/-45]_{2S}$ layup has the lowest prebuckling and postbuckling stiffnesses. Figure 6 plots the normalized load-displacement curves of composite plates with both linear and nonlinear in-plane shear formulations. The u_{xcr} is the end displacement associated with N_{xcr}. From this figure we can see that the nonlinear in-plane shear has a significant influence on the buckling and postbuckling responses for the plate with $[45/-45]_{2S}$ layup but not for the plates with $[90/0]_{2S}$ and $[45/-45/90/0]_S$ layups. This is because the plate with $[45/-45]_{2S}$ layup carries the load primary through the in-plane shear while the other two plates are less dependent on the in-plane shear to carry the loads.

Composite Plates under Biaxial Compression

In this section, the same composite plates as those in the previous section are analyzed. However, the plates in this section are subjected to uniform biaxial compressive loads with the force in the y direction being twice that in the x direction. The linearized buckling loads and buckling modes are shown in Figure 7. Again, all plates buckle into a half-wave in the x direction and a half-wave in the y direction.

The load-displacement curves of composite plates with the linear in-plane shear formulation are plotted in Figure 8. It is interesting to note that the plate with $[45/-45]_{2S}$ layup exhibits end extension before buckling occurs. For plates with $[90/0]_{2S}$ and $[45/-45/90/0]_S$ layups, the ends shorten monotonically. While the buckling load and stiffness of the plate with $[45/-45/90/0]_S$ layup is higher than those of the plate with $[90/0]_{2S}$ layup, the postbuckling loads of these two plates are about the same after a considerable amount of end shortening. Comparing Figure 8 with Figure 5, one can see that the buckling and postbuckling loads for composite plates under biaxial compressive loads are much lower than those under uniaxial compressive loads.

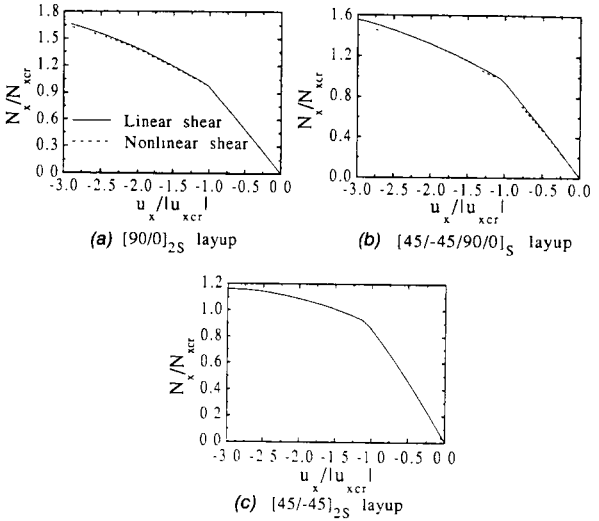

Figure 6. *Normalized load-displacement curves for composite plates under uniaxial compression with linear and nonlinear in-plane shear formulations.*

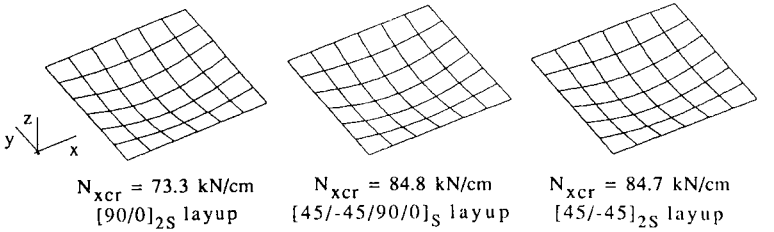

Figure 7. *Critical buckling loads and buckling modes for composite plates under biaxial compression.*

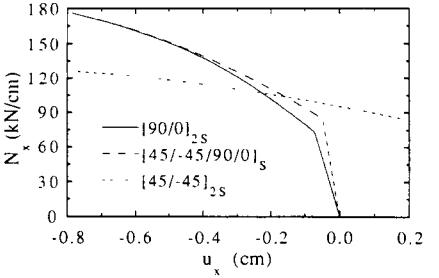

Figure 8. *Load-displacement curves for composite plates under biaxial compression with linear in-plane shear formulation.*

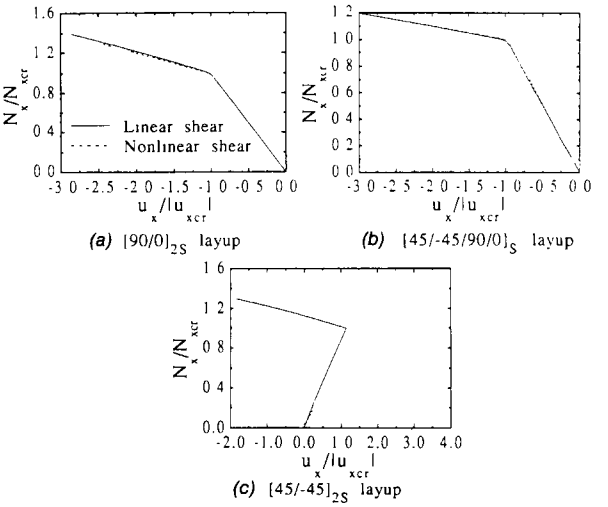

Figure 9. *Normalized load-displacement curves for composite plates under biaxial compression with linear and nonlinear in-plane shear formulations.*

Figure 9 plots the normalized load-displacement curves of composite plates with both linear and nonlinear in-plane shear formulations. From this figure we can see that the nonlinear in-plane shear has a significant influence on the buckling and postbuckling responses for the plate with $[45/-45]_{2S}$ layup. For plates with $[90/0]_{2S}$ and $[45/-45/90/0]_S$ layups, the nonlinear shear does not have much influence on their buckling and postbuckling responses. This is also because the plate with $[45/-45]_{2S}$ layup carries the load primary through the in-plane shear while the other two plates are less dependent on the in-plane shear to carry the loads.

Composite Shells under End Compression

In this section, cylindrical composite shells with different laminate layups, $[90/0]_{2S}$, $[45/-45/90/0]_S$ and $[45/-45]_{2S}$, are analyzed. Ply constitutive properties and shell geometries are given in Figure 10. These shells are subjected to uniform end compressive loads in the x direction. The edges of these shells are simply supported but allowed to move in the x direction.

The linearized buckling loads and buckling modes are shown in Figure 11. It can be seen that the buckling modes of these shells are very sensitive to laminate layups. The load-displacement curves of composite shells with the linear in-plane shear formulation are plotted in Figure 12. This figure shows that the shell with $[90/0]_{2S}$ layup has the highest prebuckling stiffness and the shell with $[45/-45/90/0]_S$ layup has the highest buckling load. For the shell with $[45/-45]_{2S}$ layup, the stiffness is much lower than those of the other two shells. Figure 13 plots the normalized load-displacement curves of composite shells with both linear and

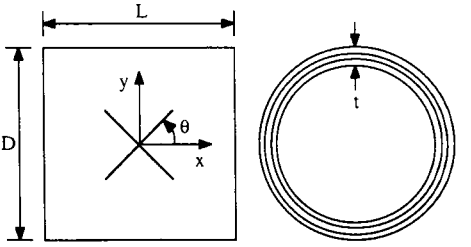

Laminate layups:
$[90/0]_{2S}$
$[45/-45/90/0]_S$
$[45/-45]_{2S}$

Composite shell geometry:
L = 20.32 cm (8 in.)
D = 20.32 cm (8 in.)
t = 1.27 cm (0.5 in.)

Ply constitutive properties:
E_{11} = 138 GPa
E_{22} = 14.5 GPa
$G_{12} = G_{13}$ = 5.86 GPa
G_{23} = 3.52 GPa
ν_{12} = 0.21
S_{6666} = 7.32 $(GPa)^{-3}$

Figure 10. *Geometries and material properties for composite laminate shell.*

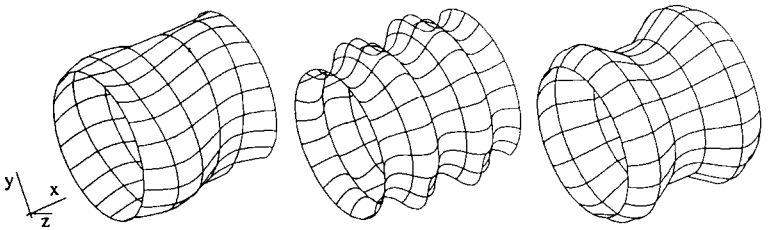

Figure 11. *Critical buckling loads and buckling modes for composite shells under end compression.*

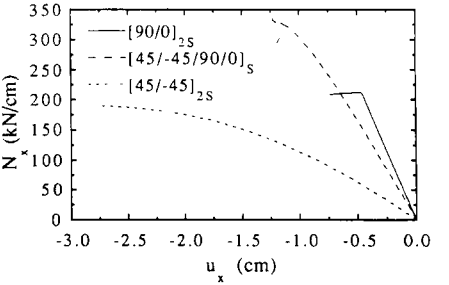

Figure 12. *Load-displacement curves for composite shells under end compression with linear in-plane shear formulation.*

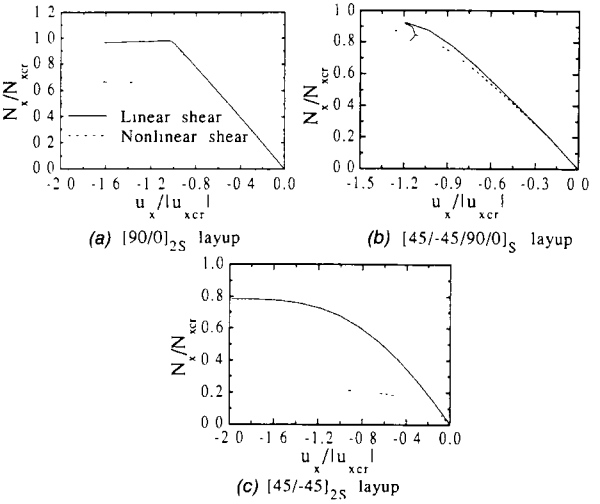

Figure 13. *Normalized load-displacement curves for composite shells under end compression with linear and nonlinear in-plane shear formulations.*

nonlinear in-plane shear formulations. From this figure one can see that the nonlinear in-plane shear has a significant influence on the postbuckling load of the shell with $[90/0]_{2s}$ layup and on the buckling responses for shells with $[45/-45/90/0]_s$ and $[45/-45]_{2s}$ layups. It is not surprising to see that the buckling behavior of the shell with $[45/-45]_{2s}$ layup calculated using the nonlinear shear formulation is much softer than that computed using the linear shear formulation since the shell with this layup carries the load primary through the in-plane shear.

Composite Shells under Hydrostatic Compression

In this section, the same composite shells are analyzed as in the previous section but they are subjected to hydrostatic compressive loads in radial and axial directions. The uniform pressure loads applied at two end surfaces are transformed into equivalent concentrated ring loads applied at two circular edges.

The linearized buckling loads and buckling modes are shown in Figure 14. Again, the buckling modes of these shells are very sensitive to laminate layups. The load-displacement curves of composite plates with the linear in-plane shear formulation are plotted in Figure 15. It is interesting to note that the shell with $[45/-45]_{2s}$ layup exhibits end extension before buckling occurs. For shells with $[90/0]_{2s}$ and $[45/-45/90/0]_s$ layups, the ends shorten monotonically. While the buckling load and stiffness of the shell with $[45/-45/90/0]_s$ layup are higher than those of the shell with $[90/0]_{2s}$ layup, the postbuckling load of the former shell is lower than the latter one after a considerable amount of end shortening. Comparing Figure 15 with Figure 12, one can see that the buckling and postbuckling

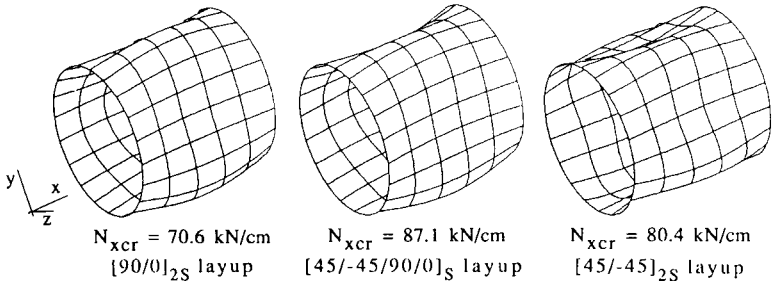

Figure 14. *Critical buckling loads and buckling modes for composite shells under hydrostatic compression.*

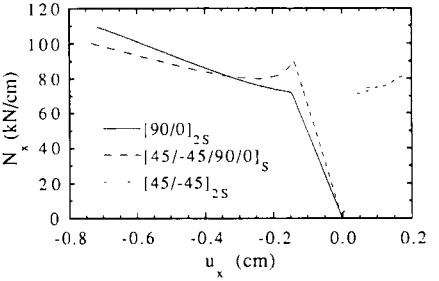

Figure 15. *Load-displacement curves for composite shells under hydrostatic compression with linear in-plane shear formulation.*

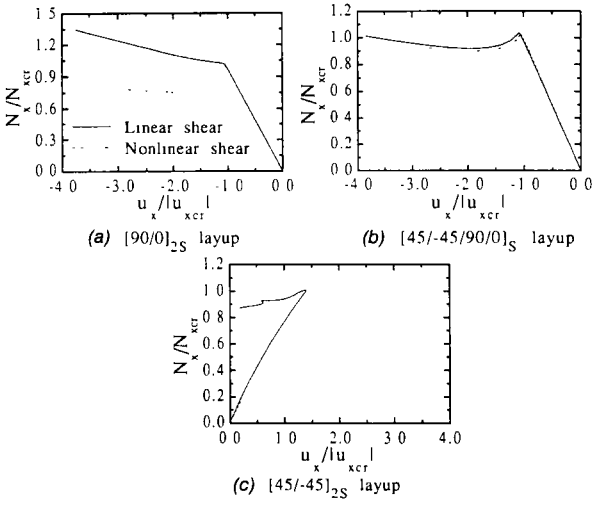

Figure 16. *Normalized load-displacement curves for composite shells under hydrostatic compression with linear and nonlinear in-plane shear formulations.*

loads for composite shells under hydrostatic compressive loads are much lower than those under end compressive loads.

Figure 16 plots the normalized load-displacement curves of composite shells with both linear and nonlinear in-plane shear formulations. From this figure we can see that the nonlinear in-plane shear has a significant influence on the postbuckling load of the shell with $[90/0]_{2S}$ layup and on both buckling and postbuckling responses of the shell with $[45/-45]_{2S}$ layup. However, it does not have much influence on the buckling and postbuckling loads of the shell with $[45/-45/90/0]_S$ layup. Again, the buckling behavior of the shell with $[45/-45]_{2S}$ layup calculated using the nonlinear shear formulation is much softer than that computed using the linear shear formulation since the shell with this layup carries the load primary through the in-plane shear.

CONCLUSIONS

From the numerical results obtained in this study, the following conclusions can be drawn:

1. The buckling and postbuckling loads for the composite plates in this study under biaxial compressive loads are much lower than those under uniaxial compressive loads. Similarly, the buckling and postbuckling loads for composite shells in this study under hydrostatic compressive loads are much lower than those under end compressive loads.
2. Under both uniaxial and biaxial compressive loads, the nonlinear in-plane shear has a significant influence on the buckling and postbuckling responses for the plate with $[45/-45]_{2S}$ layup but not for the plates with $[90/0]_{2S}$ and $[45/-45/90/0]_S$ layups.
3. Under end compressive loads, the nonlinear in-plane shear has a significant influence on the postbuckling load of the shell with $[90/0]_{2S}$ layup and on the buckling responses for shells with $[45/-45/90/0]_S$ and $[45/-45]_{2S}$ layups.
4. Under hydrostatic compressive loads, the nonlinear in-plane shear has a significant influence on the postbuckling load of the shell with $[90/0]_{2S}$ layup and on both buckling and postbuckling responses of the shell with $[45/-45]_{2S}$ layup. However, it does not have much influence on the buckling and postbuckling loads of the shell with $[45/-45/90/0]_S$ layup.

ACKNOWLEDGEMENT

The author wishes to express his appreciation to Professor Su Su Wang of the University of Houston, Texas, U.S.A., for his inspiration and fruitful discussion during the early stage of this study.

REFERENCES

1. Leissa, A. W. 1985. "Buckling of Laminated Plates and Shell Panels," Report AFWAL-TR-85-3069, Air Force Wright Aeronautical Laboratories, Wright-Patterson Air Force Base, OH.
2. Knight, N. F. and J. H. Starnes. 1985. "Postbuckling Behavior of Axially Compressed Graphite-

Epoxy Cylindrical Panels with Circular Holes," *Journal of Pressure Vessel Technology,* ASME, 107:394-402.

3. Jun, S. M. and C. S. Hong. 1988. "Buckling Behavior of Laminated Composite Cylindrical Panels under Axial Compression," *Computers and Structures,* 29:479-490.
4. Noor, A. K., J. H. Starnes and W. A. Waters. 1990. "Numerical and Experimental Simulations of the Postbuckling Response of Laminated Anisotropic Panels," *Proceedings of the 31st AIAA/ ASME/ASCE/AHS/ASC Structures, Structural Dynamics and Materials Conference, Long Beach, CA,* pp. 848-861.
5. Hahn, H. T. and S. W. Tsai. 1973. "Nonlinear Elastic Behavior of Unidirectional Composite Laminate," *Journal of Composite Materials,* 7:102-118.
6. Hashin, Z., D. Bagchi and B. W. Rosen. 1974. "Non-Linear Behavior of Fiber Composite Laminates," NASA Contractor Report, NASA CR-2313.
7. Kuppusamy, T., A. Nanda and J. N. Reddy. 1984. "Materially Nonlinear Analysis of Laminated Composite Plates," *Composite Structures,* 2:315-328.
8. Hajali, R. and S. S. Wang. 1990. "Nonlinear Behavior of Fiber Composite Materials and Its Effect on the Postbuckling Response of Laminated Plates," Report UIUC-NCCMR-90-10, National Center for Composite Materials Research, University of Illinois, Urbana, IL.
9. Sun, C. T. and J. L. Chen. 1989. "A Simple Flow Rule for Characterizing Nonlinear Behavior of Fiber Composites," *Journal of Composite Materials,* 23:1009-1020.
10. Vaziri, R., M. D. Olson and D. L. Anderson. 1991. "A Plasticity-Based Constitutive Model for Fibre-Reinforced Composite Laminates," *J. of Composite Materials,* 25:512-535.
11. Arnold, R. R. and J. Mayers. 1984. "Buckling, Postbuckling, and Crippling of Materially Nonlinear Laminated Composite Plates," *International Journal of Solids and Structures,* 20:863-880.
12. Hibbitt, Karlsson and Sorensen, Inc. 1991. *ABAQUS User and Theory Manuals, Version 4-8.* Providence, RI.
13. Mindlin, R. D. 1951. "Influence of Rotatory Inertia and Shear on Flexural Motions of Isotropic, Elastic Plates," *Journal of Applied Mechanics,* 18:31-38.
14. Irons, B. M. 1976. "The Semi-Loof Shell Element," in *Finite Elements for Thin Shells and Curved Members,* D. G. Ashwell and R. H. Gallagher, eds., London: John Wiley & Sons, pp. 197-222.
15. Riks, E. 1979. "An Incremental Approach to the Solution of Snapping and Buckling Problems," *International Journal of Solids and Structures,* 15:529-551.